https://dx.doi.org/10.1016/j.compositesa.2021.106350

Sensing Mechanism of a Carbon Nanocomposite-printed Fabric as a Strain Sensor

Xi Wang[1], Qiao Li[2,], Xiaoming Tao[3,*]*

[1]Engineering Research Center of Digitized Textile & Fashion Technology, Ministry of Education, College of Information Science and Technology, Donghua University, Shanghai 201620, China;

[2]Key Laboratory of Textile Science & Technology, Ministry of Education, College of Textiles, Donghua University, Shanghai 201620, China;

[3]Institute of Textiles and Clothing, The Hong Kong Polytechnic University, Hong Kong

**Correspondence: qiaoli@dhu.edu.cn; xiao-ming.tao@polyu.edu.hk*

Abstract

Conductive fabrics have gained widespread attention all around the electro-textile areas, owing to ease of fabrication and large freedom of design. In this paper, printed conductive knitted fabric was fabricated, which revealed favorable merits as a strain sensor such as large strain measurement range, good repeatability, good sensitivity to strain, high resistance to fatigue and low Young's modulus. The electro-mechanical behavior as well as sensing mechanism of the conductive fabric was further elaborated, based on tunneling conductive mechanism of conductive composites and gradient strain distribution of the sensing area. An electromechanical model of the conductive fabric was established and verified as effective, with maximum averaged error observed only 5.51%. The printed fabric and its model of sensing mechanism not only lay the foundation for further design, analysis and optimizations of textile-based conductive fabrics, but also reveal interesting material phenomena with a rather broad scope in the area of electronic textiles.

Keywords: A:Fabrics/textiles; A:Polymer-matrix composites (PMCs); C:Analytical modeling; D:Surface analysis

1 Introduction

Wearable electronics integrate electronic functions into a soft substrate to seamlessly contact with curved and three-dimensionally deformable human bodies [1-3]. As in soft, permeable and

deformable format, textiles are favorable dielectric supports for diverse conductors, giving rise to various components or devices such as fabric electrodes[4, 5], circuits[6], sensors[7], as well as energy harvesting[8], conversion and storage systems[9]. The conductive fabrics have been proved of being essential and effective to advance wearable electronics in vast applications such as real-time healthcare system[1, 10, 11], artificial e-skin[4, 10-14], as well as human-machine interface[15].

Conductive fabrics can be realized by two major technologies, printing electric materials on textiles [16-18] or weaving conductive yarns into fabric structures [19-21]. The printing technology have been extensively adopted on fabric substrates, due to ease of large-scale fabrication and flexible design of conductive elements in arbitrary geometries [22]. To achieve favorable extensibility (~500%) and elasticity (~100%), many efforts have been devoted to screen printing conductive materials on a knitted substrate[23], whose longitudinal (column) and transverse (row) directions are referred to as wale and course, respectively. Such created conductive knitted fabrics have made a great deal of electronic components for their own purposes [24-29], among which fabric strain sensors that respond to the stimulation of applied mechanical displacement have been frequently studied [27, 30-39]. In some experimental works, the reported sensing behaviors have reached a level comparable with or even superior than elastomeric sensors, particularly in terms of fatigue life under large deformation[26]. Compared to the large number of related researches, very few of them, however, addressed the sensing mechanisms instead of just experimental characterization [40-42]. To enhance or optimize the electromechanical behavior of those conductive fabrics as strain sensors, the relationship between electrical resistance and mechanical deformation shall be established both theoretically and experimentally.

Hence in this paper, a typical screen printed conductive knitted fabric will be made by printing carbon nanoparticles-filled silicone elastomers on a single jersey knitted fabric. The sensing mechanism of the fabric will be revealed, reflecting the resistance change of the conductive knitted fabric under tensile extension. The proposed methods and results will be representative for characterizing the distinctive material phenomena with a rather broad scope in the area of printed electronic textiles.

2 Experimental methods

2.1 Materials and fabrication.

Carbon black nanoparticles (Carbon ECP600JD, Akzo Nobel) with a weight content of 9% were fully mixed with dimethyl silicone elastomer (ELASTOSIL LR6200 A and B, Wacker Chemie AG, Germany) to form a conductive composite with a volume resistivity in the order of kOhm. Elastic knitted fabric (Sunikorn Knitters Limited, Hong Kong) comprised of polyamide filaments with a linear density of 702D/60f and spandex filaments with a linear density of 40D/4f was chosen as the substrate. The fabric density was as high as 43 courses cm^{-1} and 22 wales cm^{-1}. The conductive composite was evenly coated on the fabric with a pre-tension of 1.2N on a screen printing machine (Guangdong Ever Bright Printing Machine Fty Ltd, China). During the printing process, conductive composite was pushed and squeezed onto the fabric substrate by the squeegee through the screen mesh. Width of the conductive composite on fabric was 5mm. Later, the printed fabric was cured at 100℃ for one hour, and then gradually cooled down to the ambient temperature.

2.2 Characterization.

The specimen of conductive fabric was firstly fixed on a frame with a gauge length of 10 mm, and current-voltage characteristic curves (I-V curves) of the conductive fabric under different strains were obtained. Gauge length of the frame was increased with a step of 20% from 0 to 60%, where 60% was determined according to the average elongation scale of human skin from 3% to 55%[43]. The electrical current was measured by Solartron 1287 electrochemical interface system (Solartron Analytical, AMETEK, Inc., Hampshire, UK) under different strains with voltage gradually increased from -3 V to 3 V at a ramp speed of 100 mV/s. Then, the conductive fabric was cyclically stretched within 0~60% strain on an Instron mechanical testing system (Model 5944, Instron, USA) with electrical resistance simultaneously acquired a Keithley 2010 multimeter (Keithley instrument, USA). The tensile speed was set to 60 mm/min while the gauge length was 5 mm. All above tests were carried out under room temperature (20℃) and relative humidity of 65% RH. To track the strain distribution, white particle makers were randomly sprayed onto the surface of conductive fabric. Images of the surface speckles under different

strain levels from 0% to 60% were taken by a digital camera on an optical microscopy (Leica M165C, DFC 290HD, Leica Microsystems Ltd., Wetzlar, Germany).

3 Electromechanical property of the printed conductive knitted fabric

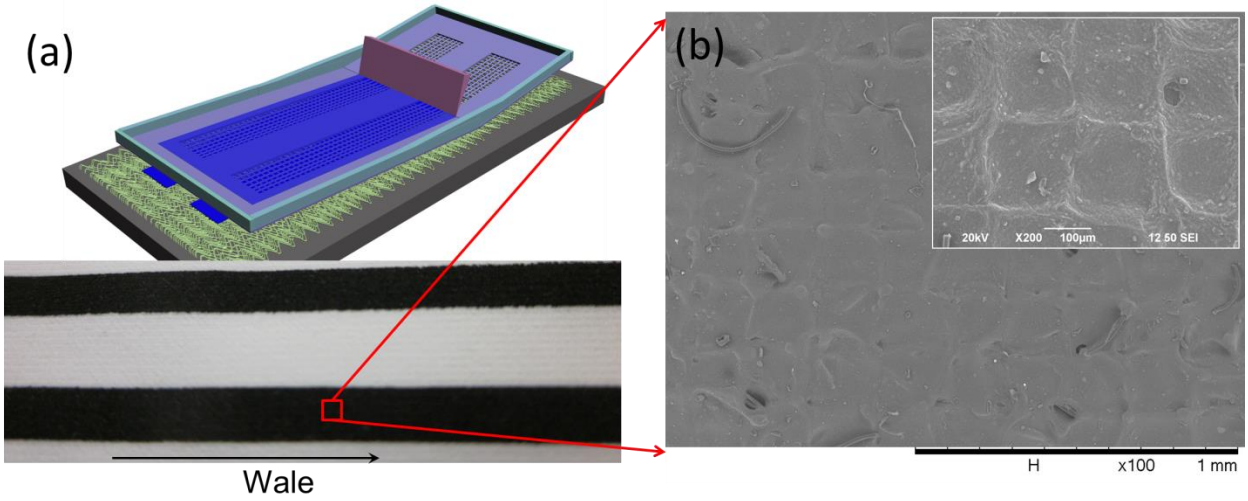

Figure 1. Carbon nanocomposite-printed fabric: (a) Screen printing process and the real picture of conductive fabric; (b) SEM image of the carbon nanocomposite surface of the conductive fabric;

The printing process (along the wale/longitudinal direction) of the conductive fabric was schematically shown in **Figure 1a**. The surface of the sensing area as in **Figure 1b** indicates that the carbon nanocomposite was continuously coated on the knitted fabric without pores, owing to the high density of the fabric substrate. The surface in gridding pattern was primarily caused by the surface waviness of the knitted structure due to the 3D looped configuration. For strains from 0 to 60% with a step of 20%, the preferred linear I-V curves of the conductive fabrics were shown in **Figure 2a**. It can be observed that a large amount of ohmic conductive pathways formed with the domination of physical contact between conductive particles or domains. The slopes of the I-V curves decreased as strain rose, suggesting that the electrical resistance increased with applied strain. These observations showed that it's feasible to use conductive fabric as strain sensor, which measures externally applied mechanical strain through the relative change of electrical conductivity. Compared to metal-based strain gauges and fiber optic/elastomeric strain sensors, the conductive fabric supports far larger working range of strain

[44]. The typical resistance-strain and tension-strain curves were shown in **Figure 2b**. It can be seen that electrical resistance rose approximately linearly from about 17.5 kΩ at 0% to 54.2 kΩ at 60%. Gauge factor (GF) can be calculated according to $GF = \frac{\Delta R / R_0}{\varepsilon}$, where ΔR and R_0 are the variation in resistance and the initial resistance, respectively, and ε is applied mechanical strain. For the obtained conductive fabric, the gauge factor was found as good as 3.5 throughout the working range of 0%~60%, indicating good sensing performance. It should be mentioned that due to mechanical relaxation of both the knitted substrate and the conductive composite, the resistance-strain relation of the 1st cycle was slightly different from the those of the later 5 extensions, which otherwise generally matched exactly with each other (**Figure 2b**). This showed that repeatability of the fabric was satisfactory from the 2nd cycle.

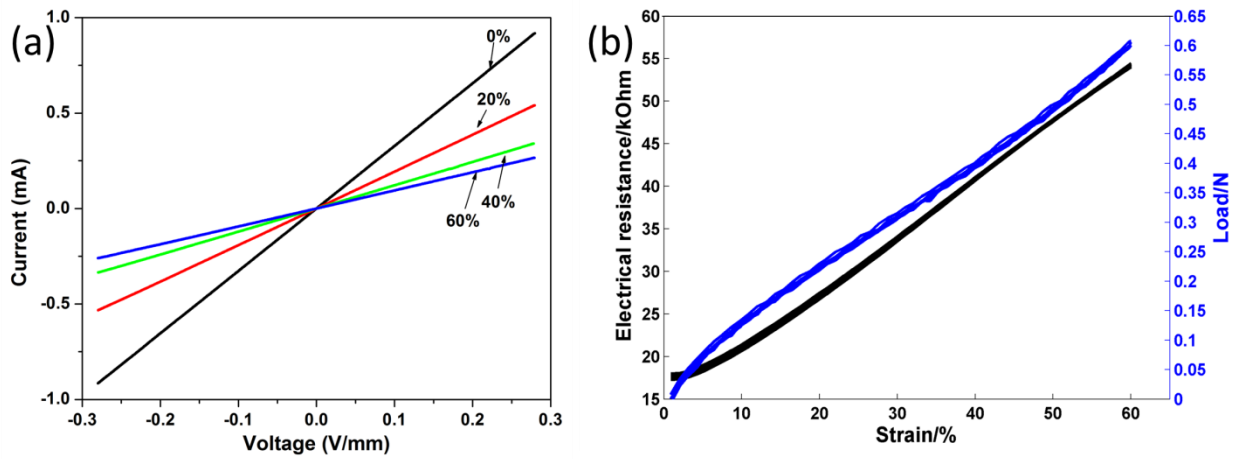

Figure 2. Electrical and electromechanical characterization of the printed conductive fabric. (a) The I-V curves under different strain levels; (b) Resistance-strain and load-strain relations obtained in cyclic tensile test.

4 Sensing mechanism

As aforementioned, the printed conductive knitted fabric consisting of knitted fabric substrate and the carbon nanocomposite as conductive material showed good strain sensing capability, hence can be utilized as strain sensors. Unlike pure conductive composites, the peculiar deformation behavior of knitted fabric has a significant impact on the strain distribution of the sensing material. Hence, to derive the electromechanical property of the conductive fabric, strain

distribution of the sensing area as well as conductive mechanism of the conductive composites shall be considered.

4.1 Plane deformation of conductive knitted fabric under extension.

Unlike printed elastomers/plastics, the printed conductive knitted fabric shows much more complicated geometrical adjustments in both wale and course cases during extension. For instance, the whole conductive fabric will not deform uniformly in uni-directional stretching case, which can be attributed to the structure and deformation behavior of the knitted substrate. As can be observed from the SEM images of front side (to be coated with conductive composite) in **Figure 3** and back side of the knitted fabric (non-coated side) in **Figure 4**), the yarn loops in the knitted fabric were initially in a jamming condition. When strain increased, yarn loops adjust their configurations through sliding and transferring between loop pillars, by which means the exerted strain in the wale direction can be accommodated. This observation is in accordance with the well-known result that the measured peak fiber strain by Raman microscope in knitted fabric is less than 1% under 30% strain [45, 46]. Thanks to the knitted structure and conversion of yarn loops, the knitted fabric exhibited peculiar plane Poisson's ratio effect unlike any pure materials, as can be indicated by the decrease of arc length with increasing strain in Figure 3f.

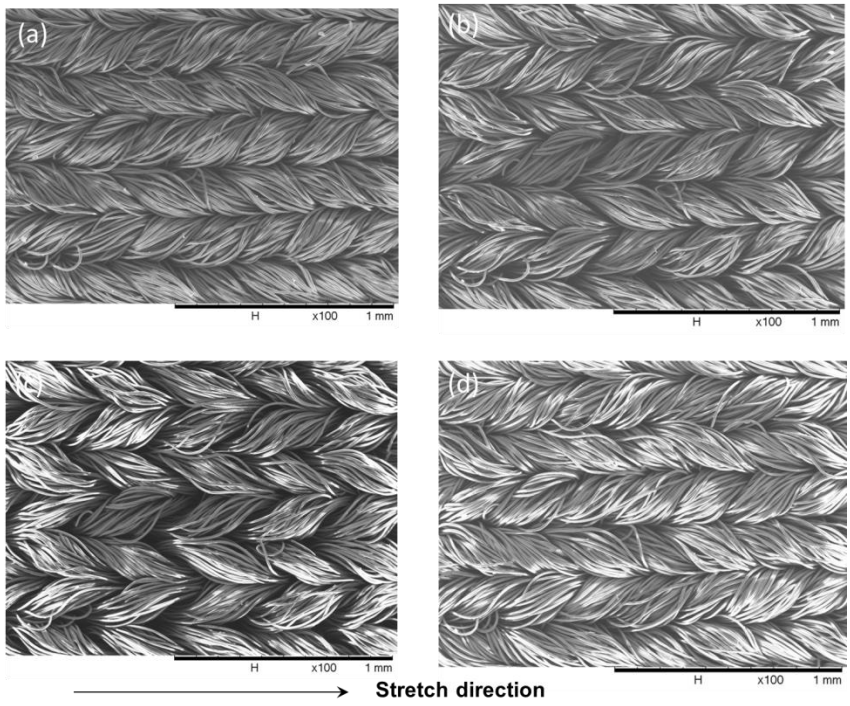

Figure 3. SEM images of geometrical change on the front side (for coating) of the knitted fabric under different strains. (a)-(d) SEM images at 0% (a), 30% (b), 60% (c), and back to 0% (d).

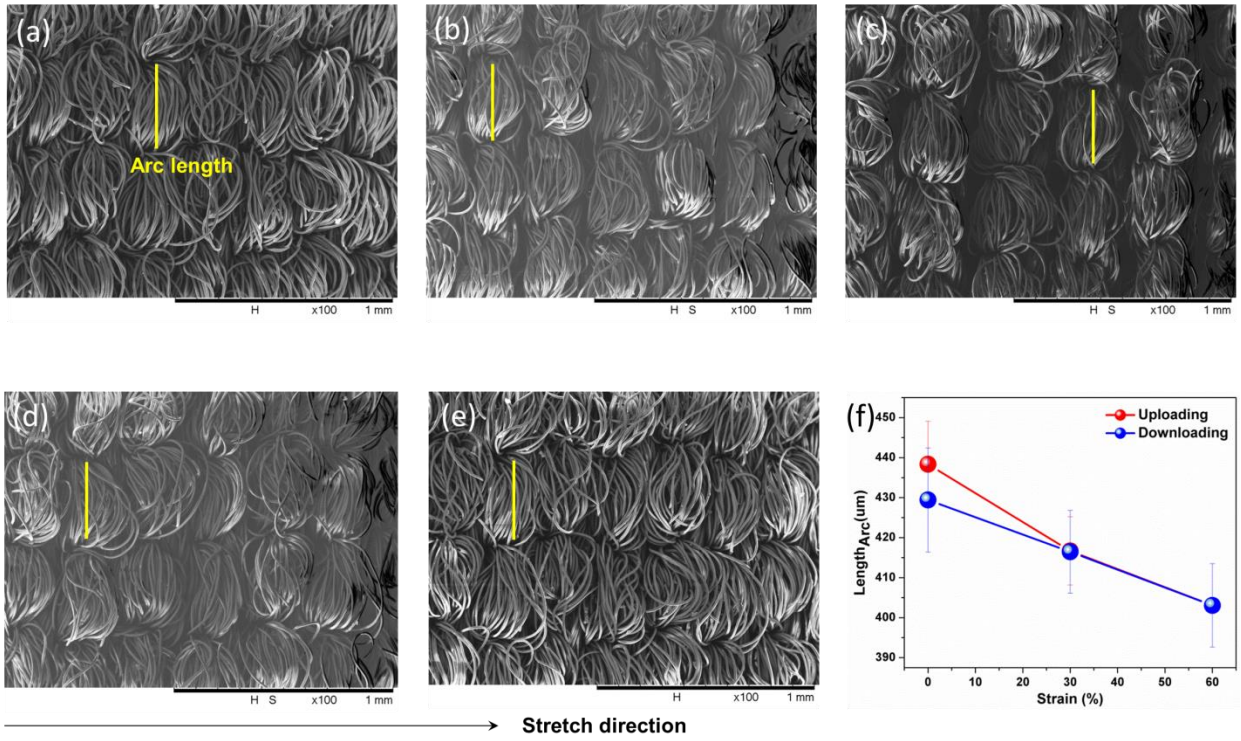

Figure 4. SEM images of geometrical change on the back side of the knitted fabric under different strains. (a-e) SEM images of the backside from 0% (a), to 30% (b), 60% (c), back to 30% (d), and back to 0% (e). (f) The variation in length of arc during tensile test, where uploading and downloading denotes the process of strain increasing and decreasing, respectively.

To quantitatively characterize the uneven and irregular deformation caused by the knitted fabric substrate, as well as the mechanical coupling between base and conductive composite, digital image correlation technique (DIC) was implemented. The sprayed marking speckles on the surface of the conductive fabric were captured by optical microscopy under different strains (**Figure 5a**), which can be further calculated to reveal the displacements along the wale direction (**Figure 5b**). It can be observed that the conductive fabric exhibited an evident but special Poisson's ratio effect, owing to the configuration and mechanical coupling between materials. For different elongation, the local strains at the wale and course cases were calculated from the

displacements of some representative marking speckles and shown in **Figure 5c-d**, respectively. The observed characteristic local strains distribution will be considered to derive the theoretical electromechanical property of the conductive fabric.

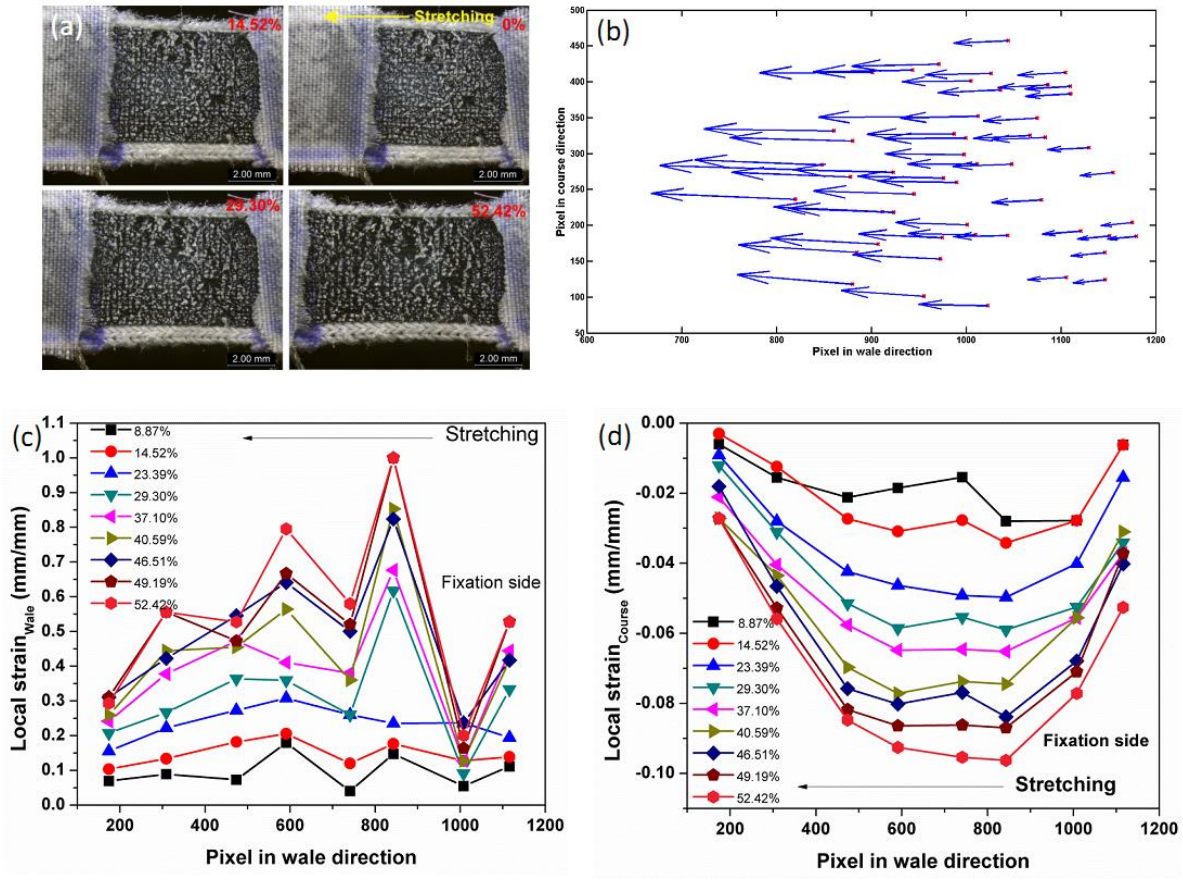

Figure 5. Plane deformation and local strains of the conductive knitted fabric during elongation. (a) Microscopic images of the coated surface under different strains from 0% to 60%. (b) Displacements of marking speckles under 30% strain. (c)-(d) Local strains in the wale and course cases, respectively.

4.2 Equivalent resistance network model of conductive fabric.

Based on the structural configuration and above characteristics of strain distribution, the conductive fabric can be separated into unit cells along the wale direction. In this condition, the electrical resistance of the printed conductive fabric can be assumed as a number of resistors connected in series, as demonstrated in **Figure 6a**. The overall resistance can be given by $R = \sum_i r_i$, where r_i is the electrical resistance of the i^{th} unit. Each unit cell can be considered

consisting of highly conductive carbon black nanoparticles with 9% weight content over percolation threshold dispersed in the flexible and insulating silicone elastomer, as can be concluded from the consistency of conductive phases indicated by the linear I-V curves in **Figure 2a**. Also, the conductivity depends not only on the relative amount of each phase present but also its degree of self-connectivity[47]. In this case, the conductive composites on the knitted substrate could properly be thought of a true conductive skeleton of a simple 3D packing geometry. For each parallel conductive pathway, conductive spheres are in spatial locations with constant angle between two adjacent ones, as shown in **Figure 6b**. If the radius of the conductive sphere is *r*, and the effective cross-sectional area through which the tunneling current passes through is $a^2 = \pi d^2$, then the center-to-center distance between two adjacent spheres *2s* can be derived as $2s = 2\sqrt{r^2 - d^2}$. The position angles θ, α, and β in **Figure 6b** hold the relation of $\cos\theta = \cos\alpha\cos\beta$. These assumptions of simplification do not adequately describe the true arrangement of conductive chains in a real composite, where the conductive pathways may meander from the straight and parallel arrangement assumed above. For comparison purposes, however, they are necessary [47]. It has been proved that resistance of the conductive composites is a function of both the resistance through each particle and the particle-particle contact resistance, including constriction resistance at the contacts, tunneling resistance at the contacts, and the intrinsic filler resistance through each particle[47-49]. Since the electrical resistance of the silicone elastomer is several orders larger than that of carbon black nanoparticles in magnitude and the distance between conductive domains is in the order of 100 Å or less, the electrical resistance of the i^{th} unit is dominated by tunneling resistance, which could be given by Simmons' equation[48, 50], i.e.,

$$r_i = \frac{L}{S}\left[\frac{8\pi h \cdot 2s}{3a^2\gamma e^2}\exp(\gamma 2s)\right] \tag{1}$$

, where $\gamma = \frac{4\pi}{h}\sqrt{2m\varphi}$, *L* the number of conductive particles forming a single conductive path parallel to the conductive direction, *S* the number of conductive pathways, *h* the Plank's constant, *e* the electron charge, *m* the electron mass, and φ the height of potential barrier between adjacent conductive particles.

4.3 Derivation of resistance-strain relationship of single unit.

According to Equation (1), the electrical resistance of the i^{th} unit rises due to the increment of distance between two adjacent conductive domains [51]. As the modulus of carbon black nanoparticles is much higher than that of silicone elastomers, the change in spatial distance between two conductive domains is mainly induced by the deformation of silicone elastomer. According to the above assumed spatial locations as in section 4.2, the initial distance between two adjacent spheres s_0 satisfies

$$s_0 = \sqrt{s_0^2 \cdot \cos^2\theta_0 + s_0^2 \cdot \cos^2\alpha_0 \sin^2\beta_0 + s_0^2 \cdot \sin^2\alpha_0} \tag{2}$$

, where α_0, β_0 and θ_0 are initial spatial angles between 2 adjacent spheres. With applied strain in the wale (length) direction, the distance s becomes

$$s = s_0 \cdot \sqrt{\cos^2\theta_0\left(1+2\varepsilon_1\right) + \cos^2\alpha_0\left(1-\cos^2\beta_0\right)\left(1+2\varepsilon_2\right) + \sin^2\alpha_0\left(1+2\varepsilon_3\right)} \tag{3}$$

, where ε_1, ε_2 and ε_3 are the corresponding local strain of the i^{th} unit in the wale, course, as well as thickness directions, respectively. Neglect the small quantity in the above equation, we have

$$\begin{aligned} s &\approx s_0 \cdot \sqrt{1+2\left(\varepsilon_1\cos^2\theta_0 + \varepsilon_2\cos^2\alpha_0 + \varepsilon_3\sin^2\alpha_0\right)} \\ &= s_0 \cdot f\left(\varepsilon_1, \varepsilon_2, \varepsilon_3, \theta_0, \alpha_0\right) \end{aligned} \tag{4}$$

Equation (4) shows that when strain is exerted, the distance between two adjacent spheres is a function of ε_1, ε_2, ε_3, θ_0, and α_0.

Please be noted that the strains ε_1, ε_2 and ε_3 along the 3 directions are not fully free, but controlled by the deformation style of the printed conductive fabric. Suppose the conductive composite is isotropic and consider a three-dimensional strain analysis. Let e_1 and e_2 be the strains exerted by knitted fabric substrate in wale and course directions, respectively; e_3 is naturally zero there is no mechanical coupling in the thickness direction. Hence, the eventual strains ε_1, ε_2 and ε_3 in the three directions satisfy

$$\begin{pmatrix} \varepsilon_1 \\ \varepsilon_2 \\ \varepsilon_3 \end{pmatrix} = \begin{bmatrix} 1 & -\nu & -\nu \\ -\nu & 1 & -\nu \\ -\nu & -\nu & 1 \end{bmatrix} \cdot \begin{pmatrix} e_1 \\ e_2 \\ 0 \end{pmatrix}$$

, where ν is the Poisson's ratio of the conductive composite. From which, we get

$\varepsilon_3 = -\nu\left(\frac{\varepsilon_1+\varepsilon_2}{1-\nu}\right)$. Eliminating ε_3 from the above equation, the function that controls the distance between two adjacent spheres can be updated:

$$\begin{aligned} f\left(\varepsilon_1,\varepsilon_2,\varepsilon_3,\theta_0,\alpha_0\right) &= \sqrt{1+2\left(\varepsilon_1\left(\cos^2\theta_0-\frac{\nu}{1-\nu}\sin^2\alpha_0\right)+\varepsilon_2\left(\cos^2\alpha_0-\frac{\nu}{1-\nu}\sin^2\alpha_0\right)\right)} \\ &= \sqrt{1+2\left(p\varepsilon_1+q\varepsilon_2\right)} \end{aligned} \tag{5}$$

, where

$$p = \cos^2\theta_0 - \frac{\nu}{1-\nu}\sin^2\alpha_0;$$

$$q = \cos^2\alpha_0 - \frac{\nu}{1-\nu}\sin^2\alpha_0;$$

Taking into account of $s^2 = r^2 - d^2$ and $a^2 = \pi\cdot d^2$, the electrical resistance of the i^{th} unit cell with applied strains could be derived, i.e.,

$$r_i = \left(\left(\frac{L}{S}\right)\cdot\frac{16h}{3\gamma e^2}\right)\cdot\frac{f}{s_0\left(g-f^2\right)}e^{2\gamma s_0\cdot f} \tag{6}$$

, where $g = \frac{r^2}{s_0^2}$.

Consequently, for the i^{th} unit, the resistance change k_i could be given by

$$k_i = \frac{r_i - r_{i0}}{r_{i0}} = \left(\frac{(g-1)f}{g-f^2}\right)\cdot e^{2\gamma s_0\cdot(f-1)} - 1 \tag{7}$$

To simplify the problem, first-order approximation is made, i.e.,

$$\begin{aligned} k_i &\approx \left(1+\left(p+G\right)\cdot\varepsilon_1+\left(q+G\right)\cdot\varepsilon_2\right)\cdot e^{2\gamma s_0\cdot\left(p\varepsilon_1+q\varepsilon_2\right)} - 1 \\ &= T\left(\varepsilon_1,\varepsilon_2,\theta_0,\alpha_0,2\gamma s_0\right) \end{aligned} \tag{8}$$

, where $2\gamma s_0 = 0.6568$ and $\nu = 0.43$, which are intrinsic characteristics of the conductive composites in this work, and the parameters p, q, G, θ_0, and α_0 hold the following relations:

$$\begin{cases} p = \cos^2\theta_0 - \dfrac{\nu}{1-\nu}\sin^2\alpha_0; \\ q = \cos^2\alpha_0 - \dfrac{\nu}{1-\nu}\sin^2\alpha_0; \\ \mathrm{G} = \dfrac{2s_0^2}{r^2 - s_0^2} \end{cases} \tag{9}$$

It can be easily seen that G was an index of distance between spheres, while p, q were the influence factors of strain in wale and course direction, respectively. For this modeling, those influence factors were exclusively determined by 3D spatial configuration in the conductive composite.

4.4 Derivation and verification of resistance-strain relation of the conductive fabric.

As aforementioned, the conductive fabric can be assumed as a continuous conductive network with a circuit of resistors connected in series. Let k_i represent the resistance change of the i^{th} unit, then the overall resistance change K of the conductive fabric under tensile extension is therefore the weighted average of that of all the unit cells, expressed by

$$K = \frac{\sum_{i=1\sim n} w_i k_i}{\sum_{i=1\sim n} w_i} \tag{10}$$

, where n denotes the number of units, which can be determined through the results of local strain as in **Figure 5c-d**. Once the resistance variation of each unit was obtained, the unknown equivalent structural parameters of the model p, q, G, θ_0 , α_0 , as well as the weight of units w_i can be fairly identified through fitting the derived model to the experimental data of different strains, in which electrical resistance was measured with digital multimeter and localized strain were captured by optical microscopy. In this work, the unknown structural parameters of one randomly chosen sample were identified as $p = 0.6; q = -0.4; G = 1.6; \theta_0 = 63^o; \alpha_0 = 46^o$ with a high fitting goodness of 0.998 (**Figure 6c**).

To verify the above methods and modeling of sensing mechanism of the conductive fabric, three more samples were adopted. Each sample was stretched by Instron 5944 to different strains, with electrical resistance measured by multimeter and local strains were obtained from surface images

simultaneously. Model of electrical resistance was then established, whose parameters were identified through above procedures. The determined mode was then used to calculate resistance variations theoretically, which were then compared to the real measured resistances for error evaluation. For all the 3 samples, a reasonably good agreement between resistance measured in experiments and that predicted by the model was observed in F**igure 6d,** with maximum averaged error observed only 5.51% (sample No.S3, at 29.3%). This result indicates that the above assumptions and methods in combined consideration of the mechanical properties of the substance fabric material and the electrical properties of the coating conductive composite was accurate and effective, which consequently laid the basis for the printed conductive knitted fabric to be further utilized as fabric strain sensor.

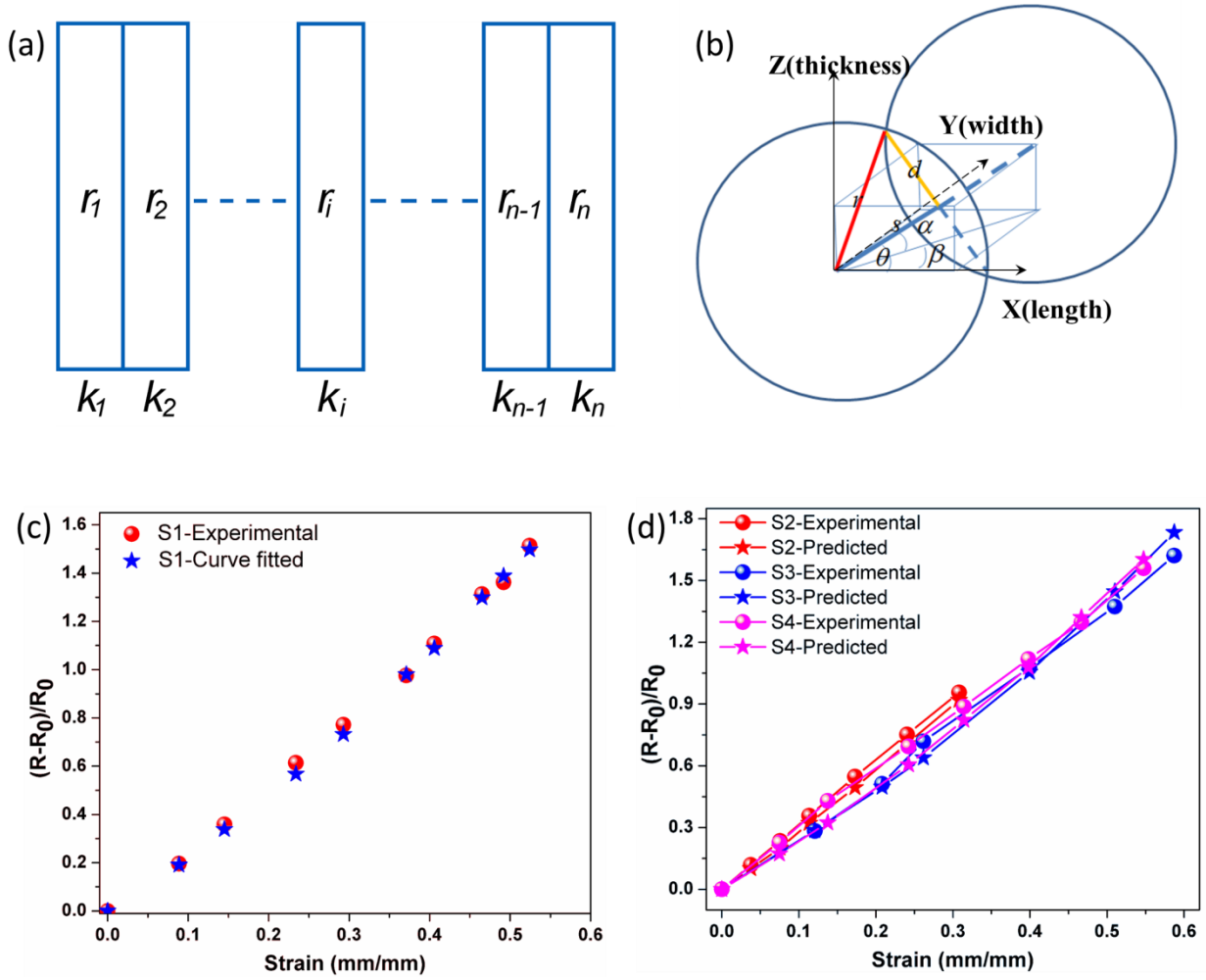

Figure 6. Modeling the sensing mechanism of the printed conductive knitted fabric. (a) Circuit

of resistors in series. (b) 3D geometric assumption of conductive spheres. (c) Determination of model parameters. (d) Model verification through comparison of measured and predicted resistance under strains.

5 Conclusion

Electronics have been integrated into textiles to have merits of being permeable, drapable in a two-curvilinear fashion and largely deformable with superior elasticity. Yet to realize accurate next-to-skin wearable applications, the sensing mechanism based on electromechanical coupling of substrate and sensing material shall also be sufficiently addressed.

In the paper, printed conductive knitted fabric was achieved by screen printing conductive nanocomposite on a knitted fabric substrate, which represents a representative type of sensing device with favorable performance for wearable applications, including large strain measurement range, good repeatability in electromechanical response, high resistance to fatigue and low Young's modulus that is comparable to human skin. Test results show that the sensor had a strain sensitivity of 3.5 with elongation up to 60% strain. Electro-mechanical behavior the conductive fabric as a fabric strain sensor was elaborated in the first place. Then, based on tunneling conductive mechanism of conductive composites and gradient strain distribution of the sensing area, the sensing mechanism and a strain-resistance model of the conductive fabric sensor was extensively derived. With determined parameters, the proposed model was tested as effective with maximum averaged error observed only 5.51%. It can be conclude that the model provided a reasonable sensing mechanism hence laying the foundation for design, analysis and optimizations of textile-based resistive conductive fabrics.

It's worth mentioning that the proposed conductive fabrics and sensing mechanism together provide a reliable option of textile electronics with a large freedom in design of conductive flexible devices, since the printed tracks may of arbitrary orientation on the fabric instead of following the yarn construction of the fabric structure.

Acknowledgement

This research was funded by the National Natural Science Foundation of China (Grant No. 12002085, 51603039), sponsored by Shanghai Pujiang Program, and supported by the

Fundamental Research Funds for the Central Universities, the Key Laboratory of Textile Science and Technology (Donghua University), Ministry of Education, as well as the Initial Research Funds for Young Teachers of Donghua University.

References

[1] H. Tian, Y. Shu, X.F. Wang, M.A. Mohammad, Z. Bie, Q.Y. Xie, C. Li, W.T. Mi, Y. Yang, T.L. Ren, A graphene-based resistive pressure sensor with record-high sensitivity in a wide pressure range, Sci Rep 5 (2015) 8603.DOI: 10.1038/srep08603.
[2] W. Zeng, L. Shu, Q. Li, S. Chen, F. Wang, X.M. Tao, Fiber-based wearable electronics: a review of materials, fabrication, devices, and applications, Adv Mater 26(31) (2014) 5310-36.DOI: 10.1002/adma.201400633.
[3] Q. Li, X.M. Tao, Three-dimensionally deformable, highly stretchable, permeable, durable and washable fabric circuit boards, Proc Math Phys Eng Sci 470(2171) (2014) 20140472.DOI: 10.1098/rspa.2014.0472.
[4] C.L. Choong, M.B. Shim, B.S. Lee, S. Jeon, D.S. Ko, T.H. Kang, J. Bae, S.H. Lee, K.E. Byun, J. Im, Y.J. Jeong, C.E. Park, J.J. Park, U.I. Chung, Highly stretchable resistive pressure sensors using a conductive elastomeric composite on a micropyramid array, Adv Mater 26(21) (2014) 3451-8.DOI: 10.1002/adma.201305182.
[5] K. Yang, C. Freeman, R. Torah, S. Beeby, J. Tudor, Screen printed fabric electrode array for wearable functional electrical stimulation, Sensor Actuat a-Phys 213(0) (2014) 108-115.DOI: 10.1016/j.sna.2014.03.025.
[6] Q. Li, L.N. Zhang, X.M. Tao, X. Ding, Review of Flexible Temperature Sensing Networks for Wearable Physiological Monitoring, Adv Healthc Mater 6(12) (2017).DOI: 10.1002/adhm.201601371.
[7] Q. Li, Y. Wang, S. Jiang, T. Li, X. Wang, Investigation into tensile hysteresis of polyurethane-containing textile substrates for coated strain sensors, Materials & design 188 (2019) 108451.DOI: 10.1016/j.matdes.2019.108451.
[8] W. Zeng, X.M. Tao, S. Chen, S.M. Shang, H.L.W. Chan, S.H. Choy, Highly durable all-fiber nanogenerator for mechanical energy harvesting, Energ Environ Sci 6(9) (2013) 2631-2638.DOI: 10.1039/c3ee41063c.
[9] K. Jost, C.R. Perez, J.K. McDonough, V. Presser, M. Heon, G. Dion, Y. Gogotsi, Carbon coated textiles for flexible energy storage, Energ Environ Sci 4(12) (2011) 5060-5067.DOI: 10.1039/c1ee02421c.
[10] D. Son, J. Lee, S. Qiao, R. Ghaffari, J. Kim, J.E. Lee, C. Song, S.J. Kim, D.J. Lee, S.W. Jun, S. Yang, M. Park, J. Shin, K. Do, M. Lee, K. Kang, C.S. Hwang, N. Lu, T. Hyeon, D.H. Kim, Multifunctional wearable devices for diagnosis and therapy of movement disorders, Nat Nanotechnol 9(5) (2014) 397-404.DOI: 10.1038/nnano.2014.38.
[11] G. Schwartz, B.C. Tee, J. Mei, A.L. Appleton, D.H. Kim, H. Wang, Z. Bao, Flexible polymer transistors with high pressure sensitivity for application in electronic skin and health monitoring, Nat Commun 4 (2013) 1859.DOI: 10.1038/ncomms2832.
[12] L.M. Castano, A.B. Flatau, Smart fabric sensors and e-textile technologies: a review, Smart Mater Struct 23(5) (2014).DOI: 10.1088/0964-1726/23/5/053001.
[13] D.J. Lipomi, M. Vosgueritchian, B.C. Tee, S.L. Hellstrom, J.A. Lee, C.H. Fox, Z. Bao, Skin-like pressure and strain sensors based on transparent elastic films of carbon nanotubes, Nat Nanotechnol 6(12) (2011) 788-92.DOI: 10.1038/nnano.2011.184.

[14] X. Wang, Y. Gu, Z. Xiong, Z. Cui, T. Zhang, Silk-molded flexible, ultrasensitive, and highly stable electronic skin for monitoring human physiological signals, Adv Mater 26(9) (2014) 1336-42.DOI: 10.1002/adma.201304248.
[15] S.C.B. Mannsfeld, B.C.K. Tee, R.M. Stoltenberg, C.V.H.H. Chen, S. Barman, B.V.O. Muir, A.N. Sokolov, C. Reese, Z.N. Bao, Highly sensitive flexible pressure sensors with microstructured rubber dielectric layers, Nat Mater 9(10) (2010) 859-864.DOI: 10.1038/nmat2834.
[16] S. Kiatkamjornwong, P. Putthimai, H. Noguchi, Comparison of textile print quality between inkjet and screen printings, Surface Coatings International Part B-Coatings Transactions 88(1) (2005) 25-34.DOI: 10.1007/Bf02699704.
[17] F. Carpi, D. De Rossi, Electroactive polymer-based devices for e-textiles in biomedicine (vol 9, pg 295, 2005), Ieee T Inf Technol B 9(4) (2005) 574-574.DOI: 10.1109/Titb.2005.858429.
[18] D. De Rossi, F. Carpi, E.P. Scilingo, Polymer based interfaces as bioinspired 'smart skins', Adv Colloid Interface Sci 116(1-3) (2005) 165-78.DOI: 10.1016/j.cis.2005.05.002.
[19] C. Zysset, T. Kinkeldei, N. Munzenrieder, L. Petti, G. Salvatore, G. Troster, Combining electronics on flexible plastic strips with textiles, Text Res J 83(11) (2013) 1130-1142.DOI: 10.1177/0040517512468813.
[20] H. Zhang, X.M. Tao, T.X. Yu, S.Y. Wang, Conductive knitted fabric as large-strain gauge under high temperature, Sensor Actuat a-Phys 126(1) (2006) 129-140.DOI: 10.1016/j.sna.2005.10.026.
[21] S. Park, S. Jayaraman, Smart textiles: Wearable electronic systems, Mrs Bull 28(8) (2003) 585-591.DOI: 10.1557/mrs2003.170.
[22] I. Kazani, C. Hertleer, G. De Mey, A. Schwarz, G. Guxho, L. Van Langenhove, Electrical Conductive Textiles Obtained by Screen Printing, Fibres Text East Eur 20(1) (2012) 57-63.
[23] B.K. Behera, B.K. Hari, Woven textile structure : theory and applications, Woodhead Pub. in association with The Textile Institute, Cambridge England, 2010.
[24] R.H. Kim, D.H. Kim, J.L. Xiao, B.H. Kim, S.I. Park, B. Panilaitis, R. Ghaffari, J.M. Yao, M. Li, Z.J. Liu, V. Malyarchuk, D.G. Kim, A.P. Le, R.G. Nuzzo, D.L. Kaplan, F.G. Omenetto, Y.G. Huang, Z. Kang, J.A. Rogers, Waterproof AlInGaP optoelectronics on stretchable substrates with applications in biomedicine and robotics, Nat Mater 9(11) (2010) 929-937.DOI: 10.1038/Nmat2879.
[25] D.L. Munden, The Geometry and Dimensional Properties of Plain-knit Fabrics, J Text I 50 (1959) T448-T471.DOI: 10.1080/19447025908659923.
[26] Y.Y. Wang, T. Hua, B. Zhu, Q. Li, W.J. Yi, X.M. Tao, Novel fabric pressure sensors: design, fabrication, and characterization, Smart Materials & Structures 20(6) (2011).DOI: 10.1088/0964-1726/20/6/065015.
[27] L. Shu, T. Hua, Y. Wang, Q. Qiao Li, D.D. Feng, X. Tao, In-shoe plantar pressure measurement and analysis system based on fabric pressure sensing array, IEEE Trans Inf Technol Biomed 14(3) (2010) 767-75.DOI: 10.1109/TITB.2009.2038904.
[28] F. Wang, B. Zhu, L. Shu, X.M. Tao, Flexible pressure sensors for smart protective clothing against impact loading, Smart Mater Struct 23(1) (2014).DOI: 10.1088/0964-1726/23/1/015001.
[29] S. Jung, J. Lee, T. Hyeon, M. Lee, D.H. Kim, Fabric-based integrated energy devices for wearable activity monitors, Adv Mater 26(36) (2014) 6329-34.DOI: 10.1002/adma.201402439.
[30] F. Wang, B. Zhu, L. Shu, X.M. Tao, Flexible pressure sensors for smart protective clothing against impact loading, Smart Mater Struct 23(1) (2014) 015001.DOI: 10.1088/0964-1726/23/1/015001.
[31] C. Zysset, N. Nasseri, L. Buthe, N. Munzenrieder, T. Kinkeldei, L. Petti, S. Kleiser, G.A. Salvatore, M. Wolf, G. Troster, Textile integrated sensors and actuators for near-infrared spectroscopy, Opt Express 21(3) (2013) 3213-3224.DOI: 10.1364/Oe.21.003213.
[32] O. Atalay, W.R. Kennon, M.D. Husain, Textile-based weft knitted strain sensors: effect of fabric parameters on sensor properties, Sensors (Basel) 13(8) (2013) 11114-27.DOI: 10.3390/s130811114.
[33] S. Coyle, K.T. Lau, N. Moyna, D. O'Gorman, D. Diamond, F. Di Francesco, D. Costanzo, P. Salvo, M.G. Trivella, D.E. De Rossi, N. Taccini, R. Paradiso, J.A. Porchet, A. Ridolfi, J. Luprano, C. Chuzel, T. Lanier, F.

Revol-Cavalier, S. Schoumacker, V. Mourier, I. Chartier, R. Convert, H. De-Moncuit, C. Bini, BIOTEX--biosensing textiles for personalised healthcare management, IEEE Trans Inf Technol Biomed 14(2) (2010) 364-70.DOI: 10.1109/TITB.2009.2038484.
[34] T. Kannaian, R. Neelaveni, G. Thilagavathi, Design and development of embroidered textile electrodes for continuous measurement of electrocardiogram signals, J Ind Text 42(3) (2013) 303-318.DOI: 10.1177/1528083712438069.
[35] E.P. Scilingo, F. Lorussi, A. Mazzoldi, D. De Rossi, Strain-sensing fabrics for wearable kinaesthetic-like systems, Ieee Sens J 3(4) (2003) 460-467.DOI: 10.1109/Jsen.2003.815771.
[36] T. Holleczek, A. Ruegg, H. Harms, G. Troster, Textile Pressure Sensors for Sports Applications, Ieee Sensor (2010) 732-737.DOI: 10.1109/Icsens.2010.5690041.
[37] S. Takamatsu, T. Kobayashi, N. Shibayama, K. Miyake, T. Itoh, Fabric pressure sensor array fabricated with die-coating and weaving techniques, Sensor Actuat a-Phys 184 (2012) 57-63.DOI: 10.1016/j.sna.2012.06.031.
[38] F. Martinez, G. Obieta, I. Uribe, T. Sikora, E. Ochoteco, Polymer-Based Self-Standing Flexible Strain Sensor, J Sensors 2010 (2010).DOI: 10.1155/2010/659571.
[39] L. Viry, A. Levi, M. Totaro, A. Mondini, V. Mattoli, B. Mazzolai, L. Beccai, Flexible three-axial force sensor for soft and highly sensitive artificial touch, Adv Mater 26(17) (2014) 2659-64, 2614.DOI: 10.1002/adma.201305064.
[40] K. Yang, R. Torah, Y. Wei, S. Beeby, J. Tudor, Waterproof and durable screen printed silver conductive tracks on textiles, Text Res J 83(19) (2013) 2023-2031.DOI: 10.1177/0040517513490063.
[41] G. Paul, R. Torah, S. Beeby, J. Tudor, The development of screen printed conductive networks on textiles for biopotential monitoring applications, Sensor Actuat a-Phys 206 (2014) 35-41.DOI: 10.1016/j.sna.2013.11.026.
[42] B. Bessais, N. Mliki, R. Bennaceur, Technological, Structural and Morphological Aspects of Screen-Printed Ito Used in Ito Si Type-Structure, Semicond Sci Tech 8(1) (1993) 116-121.DOI: 10.1088/0268-1242/8/1/019.
[43] T. Yamada, Y. Hayamizu, Y. Yamamoto, Y. Yomogida, A. Izadi-Najafabadi, D.N. Futaba, K. Hata, A stretchable carbon nanotube strain sensor for human-motion detection, Nat Nanotechnol 6(5) (2011) 296-301.DOI: 10.1038/Nnano.2011.36.
[44] A.D. Qiu, P.L. Li, Z.K. Yang, Y. Yao, I. Lee, J. Ma, A Path Beyond Metal and Silicon:Polymer/Nanomaterial Composites for Stretchable Strain Sensors, Advanced Functional Materials 29(17) (2019).DOI: ARTN 1806306

10.1002/adfm.201806306.
[45] S.W. Lam, P. Xue, X.M. Tao, T.X. Yu, Multi-scale study of tensile properties and large deformation mechanisms of polyethylene terephthalate/polypropylene knitted composites, Compos Sci Technol 63(10) (2003) 1337-1348.DOI: 10.1016/S0266-3538(02)00077-5.
[46] M. Duhovic, D. Bhattacharyya, Simulating the deformation mechanisms of knitted fabric composites, Compos Part a-Appl S 37(11) (2006) 1897-1915.DOI: 10.1016/j.compositesa.2005.12.029.
[47] G.R. Ruschau, S. Yoshikawa, R.E. Newnham, Resistivities of Conductive Composites, J Appl Phys 72(3) (1992) 953-959.DOI: 10.1063/1.352350.
[48] L.H. Wang, L.H. Cheng, Piezoresistive effect of a carbon nanotube silicone-matrix composite, Carbon 71 (2014) 319-331.DOI: 10.1016/j.carbon.2014.01.058.
[49] X.W. Zhang, Y. Pan, Q. Zheng, X.S. Yi, Time dependence of piezoresistance for the conductor-filled polymer composites, J Polym Sci Pol Phys 38(21) (2000) 2739-2749.DOI: 10.1002/1099-0488(20001101)38:21<2739::Aid-Polb40>3.0.Co;2-O.

[50] J.G. Simmons, Electric Tunnel Effect between Dissimilar Electrodes Separated by a Thin Insulating Film, J Appl Phys 34(9) (1963) 2581-2590.DOI: 10.1063/1.1729774.
[51] K.P. Sau, D. Khastgir, T.K. Chaki, Electrical conductivity of carbon black and carbon fibre filled silicone rubber composites, Angew Makromol Chem 258 (1998) 11-17.DOI: 10.1016/j.compositesa.2005.07.009.